CPI, Edificio 8E, Cubo F, 5ª planta, Camino de Vera s/n, 46022 Valencia, Spain Tel. (34) 963877270, Fax (34) 963877272, Email: energeti@upvnet.upv.es

INSTITUTO DE INGENIERÍA ENERGÉTICA
(Institute for Energy Engineering)

Research Publications

Air-side Performance of a Minichannel Evaporator under Different Dehumidifying Scenarios

Abdelrahman Hussein Hassan[1*], José Gonzálvez-Maciá[1], Santiago Martínez-Ballester[1]

[1] Universitat Politècnica de València, Institute for Energy Engineering, Camino de Vera, s/n, Valencia, 46022, Spain

[*]Corresponding author: (Tel: +34 963 879 121, E-mail: abhusab1@upvnet.upv.es)

Keywords: Minichannel Evaporator, Numerical Model, Dehumidification, Air Conditioning.

1. Introduction

Minichannel heat exchangers are used extensively these days, especially in refrigeration and air conditioning, because of many advantages such as; higher heat flux dissipation and better heat transfer coefficient, higher effectiveness, and less size and cost comparing to conventional ones. Compactness also reduces the amount of charge of the refrigerant, which has a direct positive impact on safety and environment.

When the surface temperature of the minichannel heat exchanger is below the dew point temperature of the incoming air (in the case of evaporator) the process of cooling and dehumidification is carried out. The fins of the evaporator become partially or totally wet depending on the surface temperature and inlet air properties (temperature and humidity ratio). Many experimental and numerical studies were implemented by many authors to analyze and study the performance and efficiency of the fin under dehumidification. Numerically, Liang et al. [1] presented a comparative study to investigate the wet-surface fin efficiency of a plate-fin-tube heat exchanger under a variety of fin geometric parameters and airflow conditions, especially for a wide range of air relative humidity. Their results demonstrated that In the case of partially wet surface, a considerable influence of the relative humidity on the fin efficiency is encountered. They also concluded that the 2D numerical model takes into account the complex fin geometry and the variation of moist air properties over the fin, in contrast of 1D model. Experimentally, Lin et al. [2] performed a detailed study concerning the performance of a rectangular fin in both dry and wet conditions. Their results showed that the dry fin efficiency is about 15–25 percent higher than that of the corresponding wet fin efficiency.

Currently, several minichannel evaporator models are available in the literature; most of them use the traditional ε-NTU and the adiabatic wet fin tip efficiency approach depending on the enthalpy potential which proposed by Threlkeld [3], such as; [4-6]. Although, the classical ε-NTU modeling does not account for; longitudinal conduction neither in the fin nor in the tube, transverse conduction in the tube, and the heat conduction between different tubes, which are a consequence of employing the adiabatic fin tip assumption. Emphasizing on those drawbacks, Martínez-Ballester et al. [7] developed a detailed 2D numerical model for CO_2 minichannel gas cooler to capture heat conduction effects within its structure and a detailed representation of air properties. Their study revealed large errors in capacity prediction of individual tubes due to the adiabatic fin tip assumption, especially when the neighboring tubes are at different temperatures.

In the current work, a two-dimensional numerical model for a minichannel evaporator is implemented. This model takes into account the variation of wall (fin and tube) temperature and moist air properties (temperature and humidity ratio) in both longitudinal and transverse directions. The evaporator is subdivided into segments, to which the corresponding system of mass and energy-conservation equations is applied. After validation with a well-defined analytical case, a comparative study is held between the traditional ε-NTU method and current model results under different fin conditions; totally wet, totally dry, and transition from wet to dry (partially wet).

2. Fin2D Model Development

2.1. Evaporator discretization

Fig. (1a), presents a piece of the studied minichannel evaporator. It is discretized along the X-direction (refrigerant flow) in a number of segments “a”. Each segment (Fig. 1b) consists of: two streams of refrigerant (top and bottom flows) that are split into “b” channels in the Z-direction (air flow); two flat tubes (top and bottom) that are discretized into “c” cells in the Z-direction; and both air flow and fins, which are discretized in two dimensions: “d” cells in the Y-direction and “e” cells in the Z-direction. This is summarized in the text as; grid: {a,b,c,d,e}. For illustration of the nomenclature, the numerical example shown in Fig. (1) corresponds to a grid: {2,5,3,6,5}.

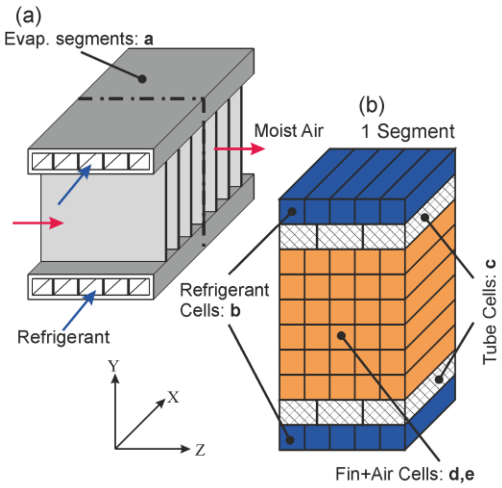

Fig. 1: (a) a piece of the evaporator under study, **(b)** schematic of the discretization in a segment of the evaporator.

2.2. Governing equations

The wall cells (tube or fin) have only one node located in the centroid of the cell, while every fluid cell (refrigerant or air) has two nodes, one at the inlet and one at the outlet. The governing equations for fluids and wall can be illustrated as following:

2.2.1. Air governing equations

The two-potential method proposed by McQuiston [8] is adopted in the current work to study the total heat transfer from the moist air. The main advantages of this method that it allows for the independent evaluation of sensible and latent heat contribution, and continuous evaluation of total heat in the transitions from humid to dry conditions. The sensible heat is evaluated based on the temperature difference between the moist air and corresponding surface wall temperature. On the other hand, the latent heat is evaluated based on the humidity ratio difference between the flowing air and the saturated air near the wall surface. The temperature variation within any air cell *i* in contact with n_i wall cells ($j=1, n_i$) is given by:

$$\dot{m}_i.\bar{C}_{p_i}.dT_i = \sum_{j=1}^{n_i} -\alpha_{ij}(\bar{T}_i - T_{s_j}).P_{ij}.ds_{ij} \tag{1}$$

where, $\bar{C}_p$ and $\bar{T}$ are the average moist air specific heat, and average air temperature within the cell, respectively. T_s is the wall surface temperature in contact with the air cell.

The mass balance within any air cell can be evaluated by the following relation:

$$\begin{aligned} \dot{m}_i.dW_i &= \sum_{j=1}^{n_i} -\alpha_{m_{ij}}(\bar{W}_i - W_{sat,s_j}).P_{ij}.ds_{ij} \quad &\text{if } (T_{s_j} < \bar{T}_{dp_i}) \\ \dot{m}_i.dW_i &= 0 \quad &\text{if } (T_{s_j} \geq \bar{T}_{dp_i}) \end{aligned} \qquad \text{where, } \alpha_{m_{ij}} = \frac{\alpha_{ij}}{Le^{2/3}.\bar{C}_{p_i}} \tag{2}$$

Chilton–Colburn analogy is used to relate the mass transfer coefficient (α_m), between the moist air and the wall surface, to the heat transfer coefficient (α) based on Lewis number (*Le*) and moist air specific heat.

2.2.2. Refrigerant governing equations

The heat balance on each refrigerant cell is evaluated by Eq. (3), which is similar to Eq. (1) but the enthalpy difference is used instead of temperature difference.

$$\dot{m}_i.dh_i = \sum_{j=1}^{n_i} -\alpha_{ij}(\bar{T}_i - T_{s_j}).P_{ij}.ds_{ij} \tag{3}$$

2.2.3. Wall governing equations

The 2D energy balance within any wall cell *j* in contact with n_j fluid cells ($i=1, n_j$) is represented by Eq. (4):

$$\nabla\left(k_{w_{j,k}}.\nabla T_{w_j}\right) + \sum_{i=1}^{n_j} \frac{1}{t_{w_j}}.\dot{q}_{ij} = 0 \tag{4}$$

where, T_w is the wall temperature evaluated at the cell centroid, $k_{w_{j,k}}$ is the thermal conductivity of the wall cell *j* in the *k* direction. The source/sink term (total heat flux) in Eq. (4) could be expressed as following:

a) if the fluid cell (*i*) is air:

$$\dot{q}_{ij} = k_{w_{j,k}}.\frac{T_{s_j} - T_{w_j}}{t_{w_j}/2} = \alpha_{ij}\left(\bar{T}_i - T_{s_j}\right) + \alpha_{m_{ij}}.h_{fg}\left(\bar{W}_i - W_{sat,s_j}\right)$$

b) if the fluid cell (*i*) is refrigerant:

$$\dot{q}_{ij} = k_{w_{j,k}}.\frac{T_{s_j} - T_{w_j}}{t_{w_j}/2} = \alpha_{ij}\left(\bar{T}_i - T_{s_j}\right) = U_{ij}\left(\bar{T}_i - T_{w_j}\right) \tag{5}$$

To linearize the source term in Eq. (5a), Elmahdy and Biggs [9] suggested a linear relation between the saturated air humidity ratio and corresponding surface wall temperature:

$$W_{sat,s_j} = a_{ij} + b_{ij}.T_{s_j} \tag{6}$$

Where *b* is the average slope of the saturation line between the wall surface temperature T_s, and surrounding air dew point T_{dp}, as proposed by Sharqawy and Zubair [10]:

$$b_{ij} = \frac{\bar{W}_i - W_{sat,s_j}}{\bar{T}_{dp_i} - T_{s_j}} \tag{7}$$

Substituting by Eq. (6) and (7) into Eq. (5a) for the saturated humidity ratio, rearranging and separating the term which depends on the wall temperature, we obtain:

$$\dot{q}_{ij} = Uw_{ij}\left(T_{ij}^{*} - T_{w_j}\right)$$

$$\text{where, } Uw_{ij} = \frac{1}{\frac{t_{w_j}/2}{k_{w_{j,k}}} + \frac{1}{\alpha_{w_{ij}}}}, \ \alpha_{w_{ij}} = \alpha_{ij}(1+\beta_{ij}.b_{ij}), \text{ and } T_{ij}^{*} = \frac{\bar{T}_i + \beta_{ij}(\bar{W}_i - a_{ij})}{1+\beta_{ij}.b_{ij}} \tag{8}$$

α_w represents the heat transfer coefficient for wet case which accounts for sensible and latent heat transfer, if there is no dehumidification then $\alpha_w=\alpha$. The overall heat transfer coefficient for wet case (Uw) accounts for total (sensible and latent) convection resistance, and conduction resistance within half thickness of the wall cell.

The LFTV numerical scheme, as explained in Corberan et al. [11] is employed for the discretization of the heat and mass transfer in Eq. (5). This numerical scheme is basically based on assuming a piecewise distribution of the fluid temperature and humidity ratio (in the case of air) along the fluid cell.

The discretization of the Laplacian operator in Eq. (4) can be made by a classical finite difference (finite volume) approach. The corresponding boundary conditions are prescribed inlet temperature and humidity ratio (in the case of air) beside the velocity distributions for both fluids, and that the open edges of the tubes to the air are considered adiabatic. The global solution method employed is called SEWTLE (for Semi Explicit method for Wall Temperature Linked Equations) and is outlined in [11].

3. Results and Discussion

3.1. Case study

In this case study, a minichannel evaporator has been modelled. Its dimensions (Table 1) are based on the evaporator tested by Zhao et al. [12], where only the tube length has been modified according to the scope of the current work.

Table 1: Geometry of the minichannel evaporator

Tube length	(cm)	8.6	Fin pitch	(mm)	1.59	Channel diameter	(mm)	1
Tube depth	(mm)	1.6	Fin thickness	(mm)	0.152	Channels number	(-)	10
Tube thickness	(mm)	0.5	Fin height	(mm)	8			

Table 2: Inlet conditions used in the simulations

	Inlet pressure (kPa)	Inlet temp. (ºC)	Inlet dew point (ºC)	Inlet quality (%)	G (kg/m^2.s)
CO_2	3600	1.4	-	22	188.76
Air	100	27	21, 16.2, 7.42, 7	-	3.34

Table (2) describes the Inlet conditions which are used in the validation of the model and numerical studies. Some data were estimated from the reported experimental data; namely, the heat transfer coefficients were estimated to be 8000 (W/m^2. ºC) for the CO_2 side and 48 (W/m^2. ºC) for the air side.

3.2. Validation of the model

Before using the newly developed model to produce detailed solutions of heat transfer in the analyzed portion of the minichannel evaporator, it is necessary to validate it. With this purpose in mind a series of systematic checks were performed against operational cases for which an analytical solution can be obtained.

The detailed discretization of the air flow in the Y-direction adopted in Fin2D makes it difficult to compare Fin2D predictions with those of analytical solutions. The validation had to consist of two steps: air side validation (V1), and fin temperature profile validation (V2). To allow a comparison against analytical solutions the following assumptions were used; the longitudinal conduction on both fin and tube walls and the transverse conduction on the tube wall were disabled, constant properties and heat transfer coefficients were used. On the other hand, conduction along the Y-direction in the fin walls was kept enabled in order to validate the calculation of heat transferred to the fins.

V1 validation is divided into two sub-validations; one for sensible heat transfer and the other for latent heat transfer. In both sub-validations the numerical solution was compared with analytical one based on single stream heat exchanger, ε=1-exp(-NTU), assuming constant tube wall temperature. Finally, the total heat transfer from air (summation of sensible and latent heat) was compared.

Fig. (2), shows the error of the numerical solution with reference to the analytical one for V1 case under totally wet and totally dry fin condition, respectively. The figure demonstrates that the error tends to diminish very quickly with the number of cells used. The abscissa shows that the number of cells in the Z-direction (air flow direction). As it can be observed, the error is very small already for N=5.

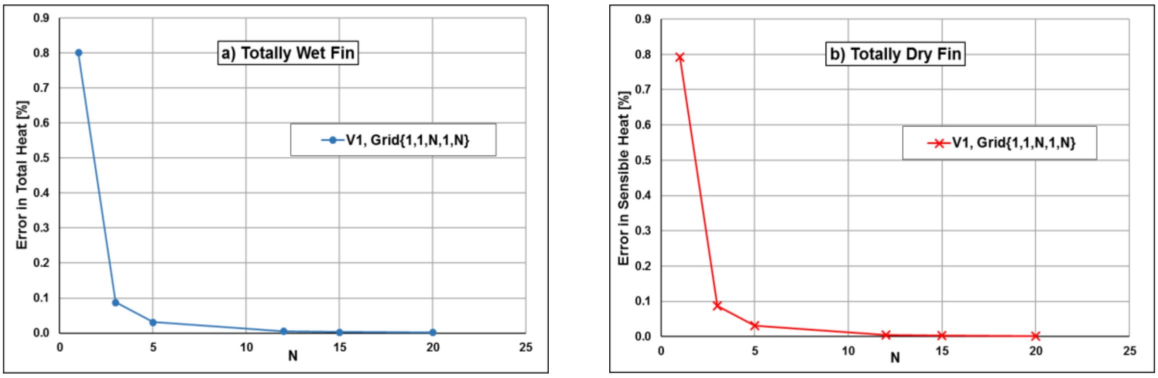

Fig. 2: V1 results for; **(a)** totally wet fin condition, **(b)** totally dry fin condition

V2 results are depicted in Fig. (3) for totally wet fin as a function of the number of cells in Y-direction, considering two situations; equal tube temperatures at the bottom and the top, and a temperature difference between tubes of 5 K. θ is the difference between the fin temperature and the air temperature. The analytical solutions for both cases have been taken from [10]. As seen from the figure, there is a very good agreement between the numerical and analytical temperature profiles, especially with increasing the number of fin cells in Y-direction.

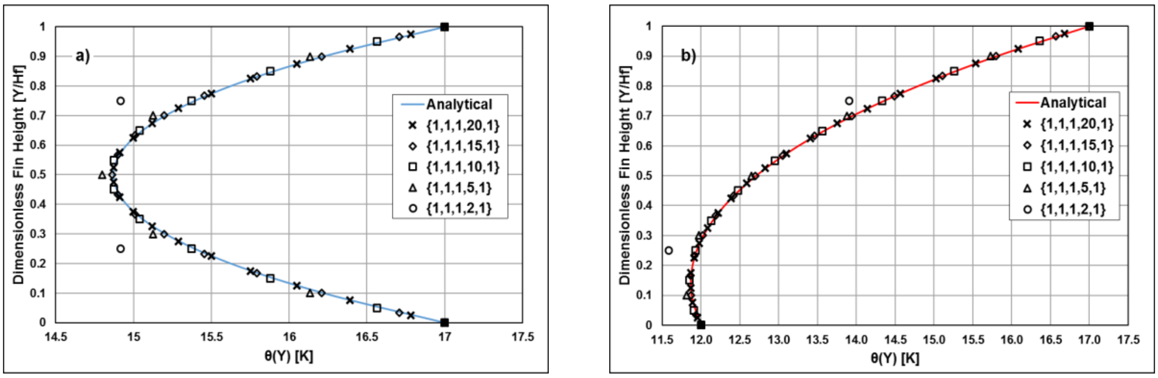

Fig. 3: V2 results for totally wet fin; **(a)** $\theta(H_f) = \theta(0)$, **(b)** $\theta(H_f) = \theta(0)+5K$

3.3. Comparative study between the classical ε-NTU method and Fin2D numerical results

Once the Fin2D model has been validated it can be used as the reference to check the deviations made by the classical segment-by-segment ε-NTU method which is widely used for modeling evaporators. The solutions to each operation scenario analyzed below were obtained with the Fin2D model using a detailed grid: {3,1,10,30,10}.

As mentioned before, most of simulation models divide each evaporator tube into segments along the refrigerant flow with its corresponding fins. Once the evaporator is divided into segments the adiabatic fin assumption and classical ε-NTU relationships for heat exchangers [13] are employed to solve the heat and mass transfer for each segment. This method simplify the solution and the calculation time, but on the other hand, it has many drawbacks, e.g. neglecting the longitudinal conduction in the tube and fin, neglecting the transverse conduction in the tube, and assuming adiabatic fin tip. These drawbacks were extensively discussed in [7]. In addition to those effects, the presence of the dehumidification process shows some other drawbacks such as:

1. *Constant air temperature and humidity ratio along the Y-direction:* besides what discussed in [7] about this topic, now constant temperature within the Y-direction results also in a constant humidity ratio in the same direction.
2. *No accounting for partially wet fin condition:* actually, depending on the fin-base temperature, the fin-tip temperature, and the dew point of the air, the fin surface can be fully dry, fully wet, or partially wet. In the ε-NTU approach, the identification of surface area below or above the dew point both along the tube and the associated fin appears to be difficult. Thus, in that approach the whole segment is usually assumed to be either completely dry or wet based on the following condition which proposed by Jiang et al. [14] and is used usually by many other authors:
   - If, $\bar{T}_w < \bar{T}_{dp}$ then the whole segment will be assumed totally wet, otherwise it will be assumed totally dry. $\bar{T}_w$ is the average wall temperature for tube and fin which calculated under dry fin condition assumption:

$$\bar{T}_w = \eta_{f_{dry}} \left(T_b - \bar{T}_a \right) + \bar{T}_a \tag{9}$$

In the current study, the tube (top and bottom) temperature was kept constant at 7 °C, while the inlet conditions for the case study in Table (2) were used to define the air status at the evaporator inlet. Those different conditions allowed us to capture different scenarios for the tube and fin. The resulted cases from the model are discussed in details and compared with classical ε-NTU approach as following.

3.3.1. *Case (I): totally wet tube and fin*

In this case, the dew point temperature of the inlet air was adjusted to 21ºC (≈ 70% RH), this situation results to a fin temperature profile below the average dew point of the air at any point, as seen in Fig. (4a).

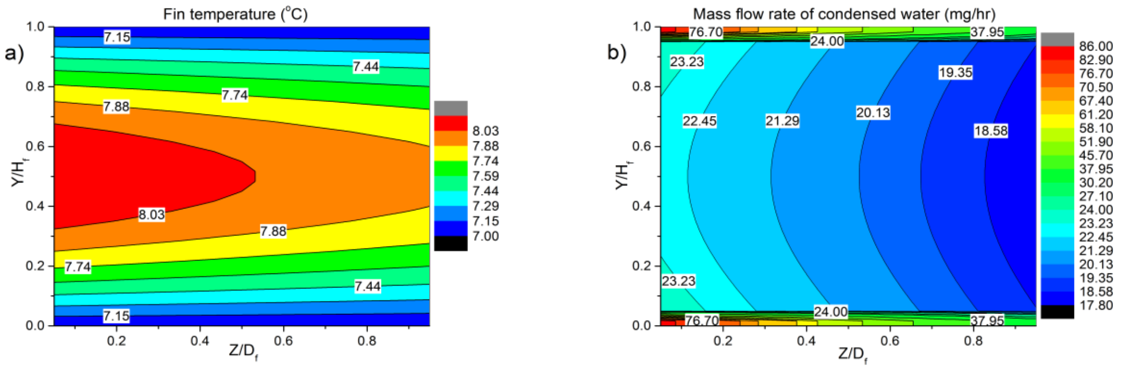

Fig. 4: (a) fin temperature profile, **(b)** mass flow rate of condensed water for case (I)

Under that condition the mass transfer due to humidity ratio difference occurs simultaneously with the heat transfer due to temperature difference, and the whole tube and fin surface becomes totally wet as depicted in Fig. (4b).

The results of ε-NTU method and current model, and the deviation in the heat transfer based on the numerical results are illustrated in Table (3). As seen in the table the traditional ε-NTU method always over estimates the amount of heat transferred. The results show almost a similar deviation in the latent and sensible heat transfer, finally the deviation in total heat between the two approaches is estimated by 3.43%.

Table 3: Deviation in the heat transfer based on numerical results, case (I)

	Fin condition	Sens. heat analysis		Lat. heat analysis		Total heat analysis	
		Q_{sens} (W)	Δ Q_{sens} (%)	Q_{lat} (W)	Δ Q_{lat} (%)	Q_{tot} (W)	Δ Q_{tot} (%)
Fin2D	Totally wet	12.46	3.53	14.37	3.34	26.83	3.43
ε-NTU		12.9		14.85		27.75	

3.3.2. *Case (II): totally wet tube and partially wet fin*

In this situation the dew point temperature of inlet air was kept at 7.42 ºC (≈ 29% RH), which is almost close to the tube surface temperature. This scenario leads to a totally wet tube. However, the numerical results have shown that there are some areas on the fin surface which have a temperature bigger than the average dew point of the corresponding air cells. So only the sensible heat is transferred between the surrounding air and those areas, resulting in a partially wet fin. Fig. (5) shows the fin temperature profile and the amount of water condensed from the air in (mg/hr), it can be noticed that nearly 40% of the fin surface is wet and the remaining is totally dry.

It can be seen in Table (4), that ε-NTU method over predicts the latent heat transfer comparing with model results, because of totally wet fin assumption. Although, the deviation in sensible heat transfer is decreased (comparing to case I), but the over prediction of latent heat increases the deviation in total heat.

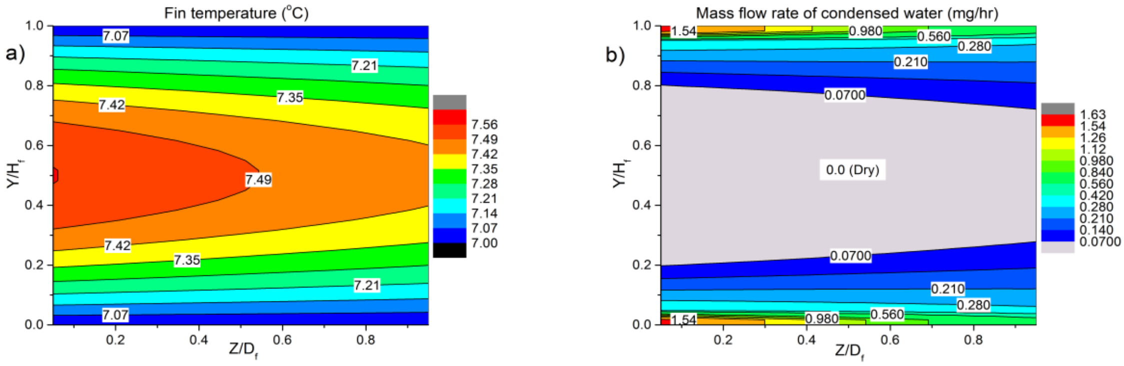

Fig. 5: (a) fin temperature profile, **(b)** mass flow rate of condensed water for case (II)

Table 4: Deviation in the heat transfer based on numerical results, case (II)

	Fin condition	Sens. heat analysis		Lat. heat analysis		Total heat analysis	
		Q_{sens} (W)	Δ Q_{sens} (%)	Q_{lat} (W)	Δ Q_{lat} (%)	Q_{tot} (W)	Δ Q_{tot} (%)
Fin2D	Partially wet	12.67	2.53	0.097	199	12.77	3.99
ε-NTU	Totally wet	12.99		0.29		13.28	

3.3.3. Case (III): totally dry tube and fin

7 °C (≈ 28% RH) dew point temperature was selected for the inlet air, which is equal to the tube surface temperature. Under this condition the tube and fin surface temperature in any location is always equal or higher than the dew point of surrounding air. This results to sensible heat transfer only and totally dry tube and fin. Table (5) demonstrates the deviation in the results, which is mainly due to the assumption of constant air temperature between tubes (drawback 1).

Table 5: Deviation in the heat transfer based on numerical results, case (III)

	Fin condition	Sens. heat analysis		Lat. heat analysis		Total heat analysis	
		Q_{sens} (W)	Δ Q_{sens} (%)	Q_{lat} (W)	Δ Q_{lat} (%)	Q_{tot} (W)	Δ Q_{tot} (%)
Fin2D	Totally dry	12.67	3.95	-	-	12.67	3.95
ε-NTU		13.17		-		13.17	

4. Conclusions

A numerical model of a minichannel evaporator under dehumidification that accounts for 2D heat conduction in any element (fin or tube), and variation of moist air properties (temperature and humidity ratio) was developed. After validation, the model was used to quantify the deviation in the heat transfer between the traditional ε-NTU approach and its numerical results under different fin conditions. The following are the main conclusions of the study:

- For totally wet fin (case I), the deviations in the latent and sensible heat between ε-NTU method and the model are very similar. The deviation in the total heat is about 3.43% and is mainly due to the assumption of constant air temperature and humidity ratio along the direction between tubes which is usually adopted in the ε-NTU approach and fin theory.
- For partially wet fin (case II), ε-NTU method fails to anticipate the fin condition because it doesn't account for partially wet scenario (drawback 2). Due to the assumption of fully

wet fin, the ε-NTU method over predicts the amount of latent heat which leads to an increase in total heat deviation by 4% comparing to the model results.

- The fin surface temperature increases (because of the release of latent heat of condensation) when there is moisture condensation. The higher the relative humidity, the higher the surface temperature becomes.
- In general, the main responsible for the deviation in results between the two approaches is the assumption of no temperature variation of the air along Y-direction which results also to a constant humidity ratio within the same direction. In reality, this assumption is not true because the temperature and humidity ratio of the air close to the tube wall and fin roots are very different than the bulk air temperature and humidity ratio. Also the assumption of only fully wet or dry fin which used usually in ε-NTU approach, although in reality the fin is partially wet, contributes in this deviation.

Nomenclature

a	parameter defined in Eq. (6)	(kg_w/kg_a)
b	parameter defined in Eq. (7)	($1/^oC$)
C_p	specific heat	($J/kg.\,^oC$)
D_f	fin depth	(m)
G	mass flux	($kg/m^2.s$)
H_f	fin height	(m)
h	specific enthalpy	(J/kg)
h_{fg}	latent heat of water condensation	(J/kg)
k	conductivity	($W/m.\,^oC$)
Le	Lewis number	(-)
$\dot{m}$	mass flow rate	(kg/s)
NTU	number of heat transfer units	(-)
P	perimeter	(m)
Q	heat transfer	(W)
$\dot{q}$	heat flux	(W/m^2)
RH	relative humidity	(%)
s	length in the direction of a fluid	(m)
T	temperature	^oC
T^*	air temp. parameter defined in Eq. (8)	^oC
t	thickness	(m)
U	overall heat transfer coefficient	($W/m^2.\,^oC$)
Uw	overall heat transfer coefficient (wet)	($W/m^2.\,^oC$)
W	humidity ratio	(kg_w/kg_a)
X,Y,Z	spatial coordinates	(m)
α	heat transfer coefficient for dry case	($W/m^2.\,^oC$)
α_m	mass transfer coefficient	($kg/m^2.s$)
α_w	heat transfer coefficient for wet case	($W/m^2.\,^oC$)
β	parameter in Eq.(8)=$h_{fg}/Le^{2/3}.C_p$	(W/m^2)
ε	thermal effectiveness	(-)
η	thermal efficiency	(-)

Subscripts

a	air
b	fin base
dry	dry surface condition
dp	dew point
f	fin
i	fluid cell index
j	wall cell index
k	direction index
lat	latent
s	wall surface
sat	saturated
sens	sensible
tot	total
w	wall centroid

θ temperature difference=T_a-T_w (ºC) or (K)

References

1. S.Y. Liang, T.N. Wong and G.K. Nathan, Comparison of one-dimensional and two-dimensional models for wet-surface fin efficiency of a plate-fin-tube heat exchanger, *Applied Thermal Engineering* 20 (2000) 941-962.
2. Y.T. Lin, K.C. Hsu, Y.J Chang and C.C. Wang, Performance of rectangular fin in wet conditions: visualization and wet fin efficiency, *ASME J. Heat Transfer* 123 (2001) 827-836.
3. J.L Threlkeld, *Thermal Environmental Engineering*, Prentice-Hall Inc., New York, 1970.
4. X.M. Wu and R.L.Webb, Thermal and hydraulic analysis of a brazed aluminum evaporator, *Applied Thermal Engineering* 22 (2002) 1369–1390.
5. Y. Zhao, Y. Liang, Y. Sun and J. Chen, Development of a mini-channel evaporator model using R1234yf as working fluid, *international journal of refrigeration* 35 (2012) 2166-2178.
6. J.J. Gossard, X. Han, M. Ramalingam and A.D. Sommers, Investigating the thermal-hydraulic performance of new refrigerant mixtures through numerical simulation of minichannel and microchannel evaporators, *Applied Thermal Engineering* 50 (2013) 1291–1298.
7. S. Martínez-Ballester, J.M. Corberán, J. Gonzálvez-Maciá and P.A. Domanski, Analysis of segment-by-segment ε-NTU modelling of a minichannel CO_2 gas cooler, *International Refrigeration and Air Conditioning Conference*, West Lafayette, USA, July 12-15, 2010.
8. F.C. McQuiston, Fin efficiency with combined heat and mass transfer, *ASHRAE Transactions* 81 (1975) 350-355.
9. A.H. Elmahdy and R.C. Biggs, Efficiency of extended surfaces with simultaneous heat transfer and mass transfer, *ASHRAE Journal* 89 (1983) 135-143.
10. M.H. Sharqawy and S.M. Zubair, Efficiency and optimization of straight fins with combined heat and mass transfer – An analytical solution, *Applied Thermal Engineering* 28 (2008) 2279–2288.
11. J.M. Corberan, P.F. De Cordoba, J. Gonzalvez and F. Alias, Semiexplicit method for wall temperature linked equations (SEWTLE): A general finite-volume technique for the calculation of complex heat exchangers, *Numer. Heat Transfer Part B-Fundam.* 40 (2001) 37-59.
12. Y. Zhao, M.M. Ohadi and R. Radermacher, Microchannel heat exchangers with carbon dioxide, Report: ARTI-21CR/10020-01 (2001).
13. F.P. Incropera and D.P. DeWitt, *Fundamentals of heat and mass transfer*, John Wiley and Sons, New York, 1996.
14. H. Jiang, V. Aute and R. Radermacher, CoilDesigner: a general-purpose simulation and design tool for air-to-refrigerant heat exchangers, *International Journal of Refrigeration* 29 (2006) 601–610.

Acknowledgement

Abdelrahman Hussein Hassan, is partially supported by Santiago Grisolía 2012 program which is funded by the Valencian Community (Generalitat Valenciana) under the reference number: GRISOLIA/2012/005. Financial support from the Spanish Ministry of Economy and Finance, project numbers: DPI2011-26771-C02-01, is also gratefully acknowledged.